

Presence of the minor allele of microRNA205 rs3842530 polymorphism increases ¹⁸FDG uptake in patients with breast cancer via targeting VEGF

SHIYING QU, TIE WANG and JINGWEI HUANG

Department of Nuclear Medicine, Beijing Chao-Yang Hospital, Capital Medical University, Beijing 100020, P.R. China

Received January 1, 2016; Accepted December 12, 2016

DOI: 10.3892/mmr.2017.7914

Abstract. MicroRNAs (miRNAs) are regarded as key regulators of gene expression involved in the pathogenesis of various diseases. Numerous single nucleotide polymorphisms (SNPs) in miRNA genes have been found to be associated with human diseases by affecting the processing process of miRNAs. In the present study, patients with breast cancer underwent a PET scan, and the maximum standard uptake value (SUV_{max})/partial volume-corrected standard uptake value (SUV_{pvc}) were determined in each individual. The samples were collected and genotyped for rs3842530. Statistical analysis was performed to evaluate the difference between the genotype groups. The results demonstrated that miR-205 downregulated the expression of vascular endothelial growth factor (VEGF) by binding to its 3'untranslated region. The introduction of exogenous miRNA, which mimicked miR-205, decreased the protein and mRNA expression levels of VEGF and, consistently, the suppression of endogenous miR-205 resulted in an increase in the expression levels of VEGF. Furthermore, it was found that the expression of mature miR-205 was markedly reduced by the presence of rs3842530. 18F-fluorodeoxyglucose (¹⁸FDG) metabolism, including SUV_{max} and SUV_{pvc}, are important parameters of PET, and dysregulation of the expression of VEGF has been reported to be associated with an altered ¹⁸FDG metabolism. In the present study, it was found that the presence of minor allele rs3842530 was correlated with increased SUV_{max} and SUV_{pvc}, which may have been mediated by release of the physiologically inhibited expression of VEGF. Therefore, VEGF was a direct target of miR-205, and the presence of rs3842530 compromised the expression of miR-205, suggesting it is a promising biomarker for the metabolism of ¹⁸FDG.

Introduction

PET with 18F-fluorodeoxyglucose (¹⁸FDG) has been applied specifically to differentiate malignant and benign nodules. Several reports have indicated that the number of patients with pulmonary nodules who receive avoidable surgical biopsies is reduced by PET (1). PET with ¹⁸FDG is a noninvasive and accurate method to diagnose single nucleotide polymorphisms (SNPs), with an overall specificity of 82% and sensitivity of 95% (2). However, in a substantial number of patients, surgical resection is required to differentiate malignant and benign nodules (3). The combining of PET and computed tomography (CT) has demonstrated superior properties in identifying a solitary pulmonary nodule (SPN) as malignant or benign, and the specificity of PET and sensitivity of CT lead to markedly enhanced accuracy overall (4).

The uptake of FDG on PET can be semi-quantitatively and qualitatively evaluated. Visual assessment, which based on comparisons of FDG uptake between the normal mediastinal blood pool and lesion is the easiest method, however, it is difficult to visually evaluate the nodules with comparable FDG uptake to the mediastinum (5). Consequently, a cut-off at the standard uptake value (SUV_{max}) is used to confirm malignancy. However, the SUV is affected by a series of factors, including lesion diameter, time following injection, blood glucose concentration and body size (6). Consequently, the SPN SUV_{max} may not represent true conditions.

As a group of non-coding small RNAs, microRNAs (miRNAs) regulate the expression of genes at the post-transcriptional level (7). miRNAs induce translational repression or mRNA degradation by targeting to the complementary sequences in the 3'untranslated regions (3'UTRs) of their target RNAs (8). Numerous studies have demonstrated that miRNAs are important in the maintenance, development and progression of diseases, including cancer (9). Accumulating evidence reports that miRNAs are involved in the progression of Ewing sarcoma, providing novel perspectives for applications in Ewing sarcoma therapy and diagnosis (10).

Hypoxia-inducible factor 1α (HIF1A)-activated transcription pathways are involved in the regulation of vascular endothelial growth factor (VEGF) genes and the expression of downstream solute carrier family 2, member 1. Under HIF1A induction-dependent hypoxic conditions, VEGF serves as the key mediator of transcription, vascular permeability and

Correspondence to: Dr Shiying Qu, Department of Nuclear Medicine, Beijing Chao-Yang Hospital, Capital Medical University, 8 South Gongti Road, Beijing 100020, P.R. China
E-mail: fdgmetabolism@163.com

Key words: microRNA-205, rs3842530, 18F-fluorodeoxyglucose metabolism, breast cancer, vascular endothelial growth factor

angiogenesis (11). VEGF plasma levels have been confirmed to be associated with a C>T polymorphism located at 936 in the 3'UTR (6). The T variant, which is associated with lower levels of VEGF, has been demonstrated to be associated with low FDG uptake (12) and colon cancer (13). These findings indicate that variants, which can alter the expression of VEGF, may be involved in the variability of FDG uptake in malignant tissues.

It has been shown that VEGF is a direct target of miR-125a in colon cancer (14,15). The rs3842530 SNP located in pri-miR-125a has been reported to compromise the processing of the mature miRNA and reduce its expression (16). Considering the role of VEGF in the determination of ^{18}F FDG metabolism, and the altered expression of miR-205 caused by the variant, the present study hypothesized that the polymorphism may be associated with ^{18}F FDG metabolism, and this was investigated in the present study by examining associations.

Patients and methods

Patients. The present study involved a total of 270 patients with breast cancer, all of which underwent a PET scan and donated 5 ml peripheral blood. All cases were diagnosed at Beijing Chaoyang Hospital Affiliated to Capital Medical University (Beijing, China) between September 2013 and December 2014. Patients suspected of breast cancer were suggested to undergo PET-CT examinations. The clinicopathological data of the participants are listed in Table I. Breast cancer tissue samples were available in 39 patients, DNA was extracted from cancer tissue samples and genotyped through direct sequencing. Written informed consent was obtained from each participant prior to the investigation. The study was performed according to the Helsinki declaration and approved by the Ethical Committee of Capital Medical University.

^{18}F -FDG PET/CT imaging. Each patient underwent FDG PET-CT examinations. In brief, the patients were weighed and fasted for 12 h prior to the PET-CT scan. The patients' blood glucose levels were also measured, and those with a blood glucose level of 150 mg/dl were excluded from the study. Each patient was intravenously injected with ^{18}F -FDG (37 MBq/10 kg; GE Healthcare Life Sciences, Little Chalfont, UK). At 1 h post-injection, the patients were instructed to raise their arms, and images were obtained from the top of the skull to the middle of the thigh via PET-CT scans, followed by a whole-body PET-CT scan (Discovery LS; GE Healthcare Life Sciences). The PET-CT protocol, including a low dose CT scan and a 3D PET whole body scan were performed at 2.5 min/bed position.

PET image quantitative analysis. Each PET image was quantitatively analyzed using Xeleris software (version 1.1363; GE Healthcare Life Sciences). PET images were initially processed and visually analyzed on sagittal, transaxial and coronal displays by three experienced technicians, who were all blind to the clinical data and the results of previous imaging studies. The circular target region was drawn to the abnormal ^{18}F -FDG-uptake-increased areas in the tumor and the standardized uptake values (including SUV_{max} and SUV_{mean}) were measured. For each slice, at least three circular (1 cm diameter) target regions were drawn from the corresponding normal

breast tissues, and the highest SUV_{max} was presented as the SUV_{max} of the normal breast tissue. The radioactivities of each tumor and normal breast tissue sample were assessed and the tumor/normal ratios were calculated.

Genotyping by direct sequencing. DNAs were extracted from homogenized cancer tissue samples and genotyped through direct sequencing. In brief, total DNA was extracted from sample tissues using a ChargeSwitch® DNA Extraction kit (Thermo Fisher Scientific, Inc., Waltham, MA, USA). The DNA extracts were then amplified through polymerase chain reaction (PCR) analysis. PCR amplification was performed on an ABI 7300 Real-Time PCR system (Applied Biosystems; Thermo Fisher Scientific Inc.) with a mixture including reverse transcription product (3 μl), forward primer (1 μl), reverse primer (1 μl), 2XSYBR-Green I Master mix (12.5 μl ; Thermo Fisher Scientific Inc.) and water (7.5 μl). The reaction settings were as follows: 20 sec at 95°C, 3 sec at 95°C, and 40 cycles of 3 sec at 95°C and 30 sec at 60°C. The primers, forward 5'-ACA GGCTGAGGTTGACATGC-3', reverse 5'-GAGTTACTCTTG CTGCTGCTG-3', were used to amplify a 247 bp fragment. The amplified samples were sent to Shanghai Shengong Biology Engineering Technology Service, Ltd. (Shanghai, China) for genotyping using a direct sequencing method.

RNA isolation and reverse transcription-quantitative PCR (RT-qPCR) analysis. Total RNA in the sample tissues and normal tissues were isolated using an RNA extraction kit (Sigma-Aldrich; Merck Millipore, Darmstadt, Germany) according to the manufacturer's protocol. The cDNA strands of target RNAs were synthesized using the high-capacity cDNA reverse transcription kit (Applied Biosystems; Thermo Fisher Scientific, Inc.) according to the manufacturer's protocol. The RNA expression was quantified and qPCR analysis was performed. PCR amplification was performed on an ABI 7300 Real-Time PCR system (Applied Biosystems; Thermo Fisher Scientific, Inc.). The relative expression of miR-205, VEGF mRNA and β -actin were determined using the $2^{-\Delta\Delta\text{Ct}}$ method (17). The PCR conditions were as follows: 2 min denaturation at 94°C, 28 cycles at 94°C for 30 sec and 58°C for 30 sec and 72°C for 40 sec. The expression of β -actin mRNA was determined as internal control.

MCF-7 cell culture and transfection. The MCF-7 cells (Chinese Cell Bank of the Chinese Academy of Sciences, Shanghai, China) were cultured 1×10^4 cell per well in Eagle's minimum essential medium (Invitrogen; Thermo Fisher Scientific, Inc.) supplemented with 20% FBS (Gibco; Thermo Fisher Scientific, Inc.) at 37°C in a 5% CO_2 environment. VEGF mimic, miR-205 mimics and scramble control mimics (GenePharma, Inc., Suzhou, China) were transfected into MCF-7 cells using Lipofectamine 2000 reagent (Invitrogen Thermo Fisher Scientific, Inc.) for 4 h at 37°C.

Bioinformatics analysis. Bioinformatics analysis was performed using online miRNA database (www.mirdb.org) (4).

Vector construction and mutagenesis. The VEGF gene -3onstr, which contains a conserved binding site for miR-205, was amplified from the human gene extracted from cancer tissue

Table I. Demographic, clinicopathological and genotypic parameters of the patients recruited in the present study.

miR205 rs3842530 genotype	INS/INS	INS/DEL + DEL/DEL	P-value
Patients (n)	165	97+8	
Sex			
Male	98	62	
Female	67	43	0.857
Age (years)	61.35±13.4	59.71±12.8	0.413
Grading			
G1/G2	111	65	
G3/G4	54	40	0.213
pT category			
T0	93	59	
T1/T2	38	28	
T3/T4	34	18	0.811
Metastases			
M (+)	37	30	
M (-)	128	75	0.621
FDG metabolism			
SUVmax	9.33±3.86	13.41±3.94	<0.001
SUVpvc	8.25±2.89	12.97±3.22	<0.001

pT, primary tumor; FDG, fluorodeoxyglucose; SUVmax, maximum standard uptake value; SUVpvc, partial volume-corrected standard uptake value; INS, insertion; DEL, deletion.

samples using PCR. The PCR products were subcloned into the pmiR-RB-REPORTTM vector (Promega Corporation, Madison, WI, USA). In addition, mutant fragments were generated from mutagenesis and introduced into the same sites of the control vector.

Luciferase assay. The VEGF gene -3' se as, which contains a miR-205 binding site, was amplified from the human gene using PCR. PCR amplification was performed on an ABI 7300 Real-Time PCR system (Applied Biosystems; Thermo Fisher Scientific, Inc.) with a mixture including reverse transcription product (3 μ l), forward primer (1 μ l), reverse primer (1 μ l), 2XSYBR-Green I Master mix (12.5 μ l; Thermo Fisher Scientific, Inc.) and water (7.5 μ l). The reaction setting were as follows: 20 sec at 95°C, 3 sec at 95°C, 40 cycles of 3 sec at 95°C and 30 sec at 60°C. The primers used to amplify VEGF were: Forward: 5'-CCTTTGGGTTTTGCCAGA-3' and Reverse: 5'-CCAAGTTTGTGGAGCTGA-3'. The PCR products were subcloned into the pmiR-RB-REPORTTM vector (Promega Corporation). Mutant fragments were also generated from mutagenesis and introduced into the same sites of the control vector. For the analysis of luciferase activity, MCF-7 cells were seeded 1x10⁴ cell per well in 96-well plates overnight prior to transfection. The cells were cotransfected with miR-205 mimic/mimic control and wild-type/mutant vector (Promega Corporation) using the Lipofectamine 2000 Transfection system (Invitrogen; Thermo Fisher Scientific, Inc.). At 48 h post-transfection, luciferase activity was measured using the Dual-Luciferase Reporter Assay system (Promega Corporation) according to the manufacturer's protocol. A

Renilla luciferase plasmid was used as an internal control. Each experiment was repeated three times.

Western blot analysis. Western blot analysis was performed to determine the protein expression levels of miR-205 and VEGF in the sample tissues and cultured cells. The sample tissues were rinsed with 4°C PBS (Beijing Zhongshan Golden Bridge Biotechnology Co., Ltd., Beijing, China) and total proteins were extracted using cell lysis buffer, which contained 50 mmol/l Tris HCl, 150 mmol/l NaCl, 0.1% SDS, 100 μ g/ml phenylmethylsulfonyl fluoride, 1% NP-40 and 1 μ g/ml aprotinin (pH 8.0). The concentrations of protein extracts were determined using the Bradford method. The protein extracts (30 μ g) were loaded on 10% SDS-PAGE gels. Following electrophoresis, the proteins were transblotted onto nitrocellulose membranes (Bio-Rad Laboratories, Inc., Hercules, CA, USA). The blots were then blocked and washed to avoid unspecific binding. The membranes were then incubated with primary antibodies (anti-VEGF antibody; sc-4570; 1:1,000; anti- β -actin antibody; sc-418965; 1:10,000) and secondary antibody (sc-51948; 1:10,000; all from Santa Cruz Biotechnology, Inc.). The bands were visualized by chemiluminescence (ECL-Plus; Santa Cruz Biotechnology, Inc.).

Statistical analysis. Statistical analysis was performed using the Statistical Package for the Social Sciences software (SPSS) for Windows 13.0 (SPSS, Inc., Chicago, IL, USA). The data for SUVmean, SUVmax and tumor/normal are expressed as the mean \pm standard deviation, and a two-sample t-test was used for comparison between tumors and normal tissues. A χ^2 test

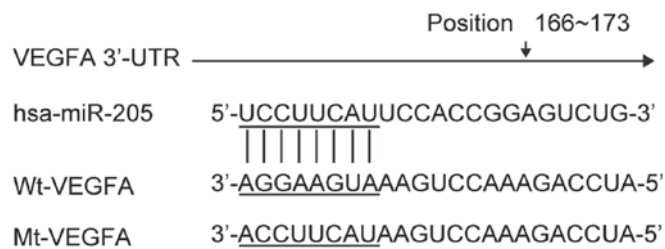


Figure 1. Predicted target sequence of miR-205 within the human VEGF 3'UTR. The predicted seed regions are underlined. Mutation was introduced through destruction of the seed regions. 3'UTR, 3'untranslated region; VEGF, vascular endothelial growth factor; miR, microRNA; wt, wild-type; mut, mutant.

was performed to compare categorical data in different groups. The odds ratios and 95% confidence intervals were calculated using univariate and multivariate logistic regression analyses to determine potential associations. Differences between the groups were determined using a Mann-Whitney test for nonparametric data. Group differences for dichotomous data were determined using a χ^2 test or Fisher's exact test. $P < 0.05$ was considered to indicate a statistically significant difference.

Results

miR-205 represses the expression of VEGF. Using bioinformatics analysis, miR-205 was predicted to target the human VEGF 3'UTR at position 166-173 (Fig. 1). To investigate whether the expression level of miR-205 was correlated with the expression level of VEGF, luciferase reporter vectors were constructed, which contained a wild-type or mutated VEGF 3'UTR downstream of Firefly luciferase (Fig. 1). The miR-205 mimic and reporter vectors were co-transfected into MCF-7 cells. A dual-luciferase assay was performed 48 h post-transfection. The results of the dual-luciferase assay showed that when the reporter vector contained a wild-type VEGF 3'UTR, miR-205 suppressed the expression of luciferase. By contrast, mutation of the seed regions completely eliminated this inhibition (Fig. 2). These results showed that miR-205 targeted the VEGF 3'UTR directly and suppressed the expression of VEGF.

To determine whether miR-205 disrupted the endogenous expression of VEGF in breast cancer cells, miR-205 mimics were transfected into MCF-7 cells, with blank and scramble as negative controls, and VEGF small interfering (si)RNA as a positive control. The data showed that mRNA and protein expression levels of VEGF were suppressed by the miR-205 mimic (Fig. 3A and B). Similar experiments were performed involving miR-205 inhibitor treatment, and the decrease of miR-205 increased the mRNA and protein levels of VEGF (Fig. 3A and B).

Rs3842530 decreases the expression of VEGF via miR-205. An SNP exists in the miR-205 gene, termed rs3842530. To investigate whether the expression of miR-205 can be eliminated by this SNP in breast cancer, the present study compared the expression levels of miR-205 in a number of breast tumor tissue samples with different miR-205 genotypes. The results showed that the expression level of miR-205 was reduced in

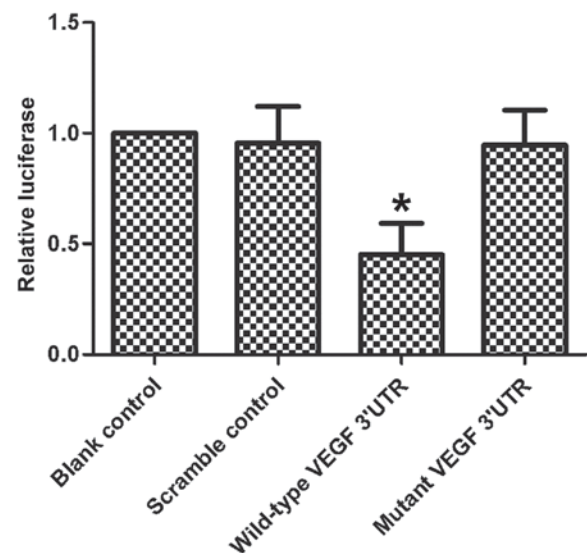


Figure 2. miR-205 can target the VEGF 3'UTR. Scramble or miR-205 mimics were co-transfected with luciferase reporter vectors containing VEGF wild-type or mutant 3'UTR, respectively. Luciferase activity was measured at 48 h post-transfection. Each data point was measured in triplicate. The data were normalized to the ratio of Firefly and Renilla luciferase activities, measured at 48 h post-transfection. Results are presented as relative luciferase activity in which the control was assigned a value of 1. Values are presented as the mean \pm standard deviation from three independent transfection experiments. miR-205 only inhibited luciferase activity of wild type VEGF 3'UTR, but not that of mutant VEGF 3'UTR ($P < 0.05$ vs. scramble control). * $P < 0.05$. 3'UTR, 3'untranslated region; VEGF, vascular endothelial growth factor; miR, microRNA.

samples containing rs3842530 (Fig. 4A). It was hypothesized that a reduction of miR-205 mediated by rs3842530 leads to a further increase in the expression of VEGF. To evaluate this, RT-qPCR analysis was used to determine the mRNA expression level of VEGF. In addition, western blot analysis was used to determine the protein expression level of VEGF (Fig. 4B and C). The results showed that the mRNA and protein levels of VEGF were significantly increased in samples with rs3842530 (Fig. 4B and C). Of note, the changes in miR-205 and the level of VEGF were inversely correlated.

Rs3842530 affects ¹⁸FDG metabolism mediated by miR-205 and VEGF. Correlation analyses were performed to determine whether rs3842530 was associated with certain breast tumor characteristics. It was found that patients with the minor allele of rs3842530 had significantly higher SUVmax and SUVpvc values, compared with patients with a wild-type genotype (Table I). As is already known, SUVmax and SUVpvc are important parameters in ¹⁸FDG-PET analysis, and they can be used to reflect glucose metabolism. A previous study showed that a high level of glucose metabolism is an important characteristic in malignant tumors and that dysregulation of the expression of VEGF has been reported to be associated with altered glucose metabolism (4). Consequently, the present study hypothesized that patients with the minor allele of rs3842530 have associated higher glucose metabolism. These data suggested that the minor allele of rs3842530 accelerated glucose metabolism by compromising the expression of miR-205, which indicates it as a promising biomarker for the metabolism of ¹⁸FDG.

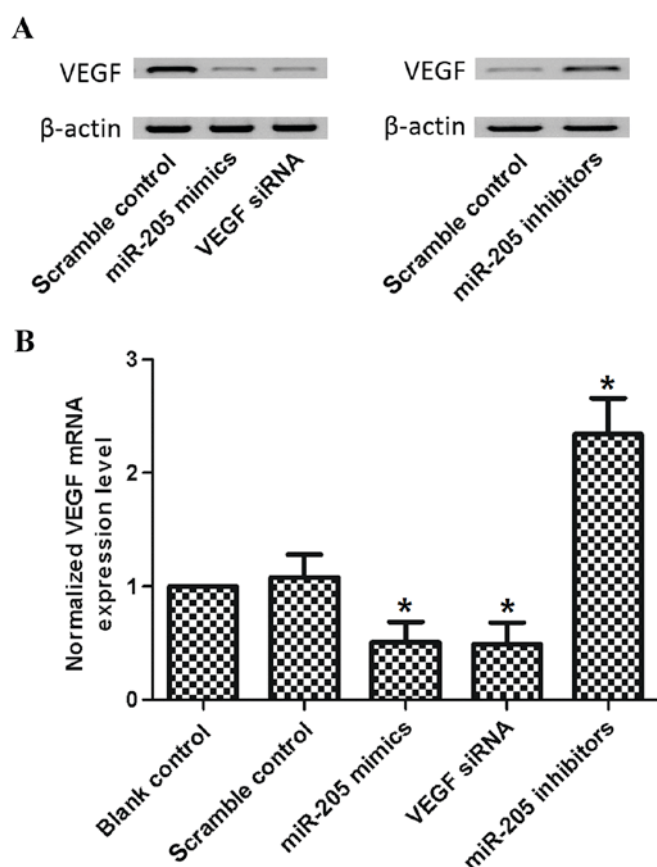


Figure 3. Protein and mRNA levels of VEGF can be inhibited by miR-205. miR-205 mimics or inhibitor were transfected into MCF-7 cells, respectively. (A) Western blot analysis was used to analyze the protein levels of VEGF. miR-205 and VEGF significantly inhibited VEGF protein expression ($P < 0.05$ vs. scramble control), while miR-205 inhibitor evidently enhanced VEGF protein expression ($P < 0.05$ vs. scramble control). (B) Relative mRNA expression levels of VEGF were determined using reverse transcription-quantitative polymerase chain reaction analysis. miR-205 and VEGF significantly reduced VEGF mRNA expression ($P < 0.05$ vs. scramble control), while miR-205 inhibitor evidently increased VEGF mRNA expression ($P < 0.05$ vs. scramble control). A blank control and scramble control were used as negative controls. VEGF siRNA was used a positive control. Values are presented as the mean \pm standard deviation. miR, microRNA; VEGF, vascular endothelial growth factor; siRNA, small interfering RNA.

Discussion

As non-coding small RNAs, miRNAs negatively regulate the expression of genes via the degradation of mRNA or via translational repression. In humans, >700 miRNAs have been identified and registered, and each of these can bind to several genes on the bases of the seed sequence matches in their 3'UTRs (18). miRNAs are involved in pathologic and biological processes, including cell apoptosis, proliferation, differentiation and metabolism (19), and they have shown potential as tissue-specific biomarkers, which may be used to identify cancer origin and type (20). Increasing evidence demonstrates that the deregulation of miRNAs is involved in human cancer, and suggests a causative role of miRs in cancer progression and initiation as they can serve as tumor suppressors or oncogenes (21). Marked differences in the expression patterns of miRNAs have been reported among adenocarcinoma, in esophageal and squamous cell carcinoma and in other types of cancer (22). High expression levels

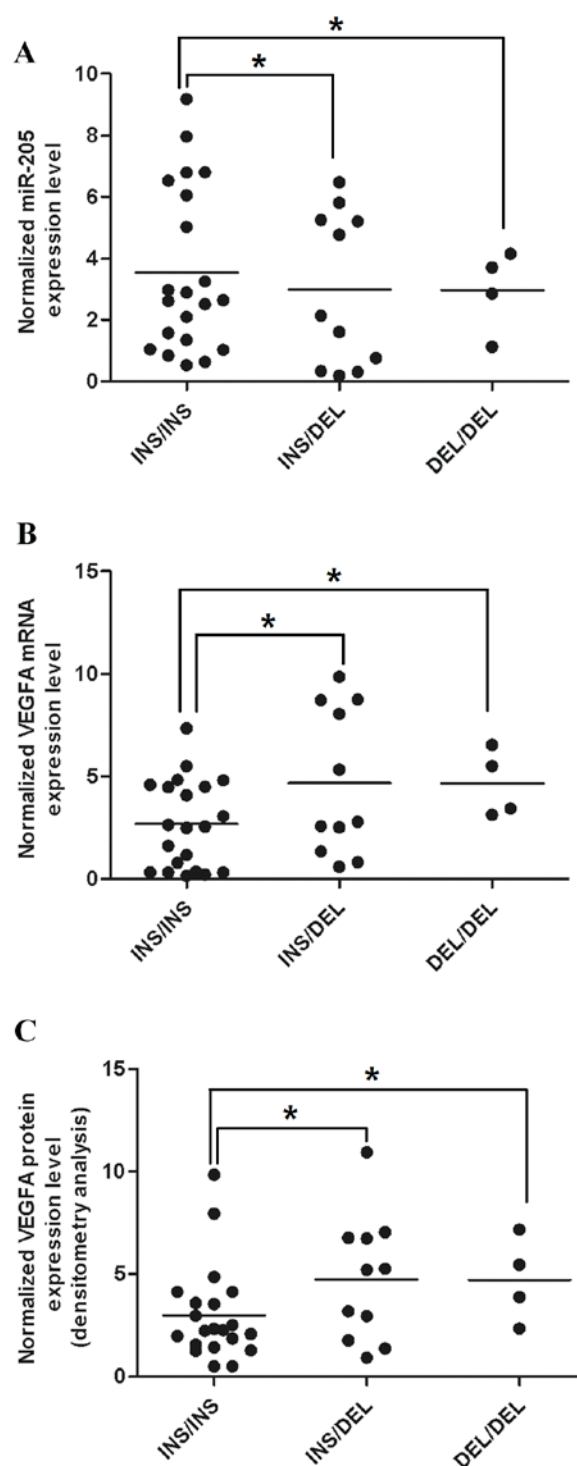


Figure 4. DEL can reduce the expression level of miR-205 and increase the expression level of VEGF. The expression levels of (A) mature miR-205 ($P < 0.05$ vs. INS/INS group), (B) VEGF mRNA ($P < 0.05$ vs. INS/INS group) and (C) VEGF protein ($P < 0.05$ vs. INS/INS group) (INS/INS, 21; INS/DEL, 11; DEL/DEL, 4). Single DEL resulted in the reduced expression level of mature miR-205, thereby releasing the expression of its target gene, VEGF. miR, microRNA; VEGF, vascular endothelial growth factor; INS, insertion; DEL, deletion.

of miR-205 in malignant and benign squamous epithelia, including esophageal squamous cell carcinoma (ESCC), were reported by Kimura *et al* (23), whereas the expression level was lower in tissues and cell lines other than squamous epithelia. By contrast, the expression level of miR-21, which

acts as an oncogenic miRNA in several types of cancer, was induced in ESCC, compared with paired normal squamous epithelia. However, elucidation of the roles of functional VEGF specific-miRs remained limited (23). In the present study, it was predicted that miR-205 targeted the human VEGF 3'UTR at position 166-173 using bioinformatics analysis (Fig. 1). Additionally, a dual-luciferase assay was performed, which found that in reporter vectors containing a wild-type VEGF 3'UTR, miR-205 suppressed the expression of luciferase. By contrast, seed region mutations completely eliminated this inhibition (Fig. 2). These results confirmed that miR-205 targeted the VEGF 3'UTR directly.

VEGF serves as an essential factor in the angiogenesis of tumors, and VEGF pathway activation requires the binding of ligands, including VEGFA, to one of its receptors, including kinase insert domain receptor (KDR) or fms-like tyrosine kinase 1 (FLT1). Consequently, downstream signals are generated to stimulate the structural reorganization and proliferation of endothelial cells (24). There are four members in the VEGF family, including VEGFD, VEGFC, VEGFB and VEGFA, and VEGF receptors are comprised of three subtypes, including VEGFR3, VEGFR2 (KDR) and VEGFR1 (FLT1) (25). VEGFA acts as major regulator in the development of angiogenesis and vasculogenesis, predominantly by interacting with KDR and FLT1 to produce downstream signaling (25). As a tyrosine kinase receptor, FLT1 demonstrates ~10-fold higher affinity, compared with KDR in binding VEGFA. Although VEGF ligands poorly activate FLT1, it has been found to accelerate tumor metastasis and growth (25). By contrast, potent downstream signals are induced when the VEGF ligand binds KDR, leading to endothelial cell migration and growth (25). There has been limited success in targeted therapy for malignant glioma due to the converging complex interactions and parallels among certain critical pathways, including pathways involved in the regulation of angiogenesis of tumors (26). In the present study, miR-205 mimics were transfected into MCF-7 cells, with blank and scramble as negative controls, and VEGF siRNA as a positive control. The data showed that the mRNA and protein expression levels of VEGF were suppressed by the miR-205 mimic (Fig. 3A and B). Similar experiments were performed using miR-205 inhibitor, and the decrease in miR-205 increased the mRNA and protein levels of VEGF (Fig. 3A and B).

SNPs are risk factors of breast cancer as nine large genome-wide association studies reported (27). However, the commercial exploitation of SNPs in clinical use remains controversial despite considerable progress (28). Further investigations are required to investigate the potential functional effect of specific SNPs on PET uptake in human cancer. A previous study was performed involving 37 patients with breast cancer without metastases, which demonstrated the association between FDG uptake in breast cancer and a human SNP (rs3025039 of VEGFA) (12). miRs have been identified as gene regulators, which are expressed at aberrant levels and are involved in virtually all subtypes of cancer (29). miRs target the 3'UTR of target genes, regions which show a high level of evolutionarily conservation (30), indicating the importance of these regions in natural selection. As each miRNA manipulates numerous mRNAs at

the same time (31), the potential for cellular transformation originating from a single miRNA dysfunction is high. The roles of the miRNA SNPs in disorders have been identified and their importance has been confirmed. miR-125a, which shows aberrant expression levels in breast cancer (32) has an SNP variant allele in the mature miRNA sequence, which reduces the expression level (33). It has been demonstrated that SNPs in binding sites of RNAs may be associated with disease, for example, miR-189 binding is disrupted by a point mutation located in the 3'UTR of SLIT and NTRK like family member 1 in certain patients with Tourette's syndrome (34). In addition, SNPs in miRNA target spots in human cancer genes were reported in a study in which differences in allele frequencies between normal and cancerous tissues were found (35). Finally, it has been reported that an SNP existing in the binding site of miRNA in the kit oncogene was associated with induced expression of genes in papillary thyroid cancer (36). In the present study, breast cancer tissue samples were collected and genotyped for rs3842530 (37). It was found that the expression level of miR-205 was reduced in samples containing rs3842530 (Fig. 4A), and the mRNA and protein levels of VEGF were significantly increased in samples with rs3842530 (Fig. 4B and C). Furthermore, an association experiment was performed in the breast cancer patient population (n=270), and it was identified that patients with the minor allele of rs3842530 had significantly higher SUVmax and SUVpvc, compared with those patients with a wild-type genotype (Table I).

Taken together, the findings of the present study showed that VEGF was a direct target of miR-205 and the presence of rs3842530 reduced the expression of VEGF, rs3842530 was associated with ¹⁸FDG metabolism in patients with breast cancer and may be a promising biomarker for PET scan parameter predictions.

References

1. Nomori H, Watanabe K, Ohtsuka T, Naruke T, Suemasu K and Uno K: Visual and semiquantitative analyses for F-18 fluorodeoxyglucose PET scanning in pulmonary nodules 1 to 3 cm in size. *Ann Thorac Surg* 79: 984-989, 2005.
2. Cronin P, Dwamena BA, Kelly AM and Carlos RC: Solitary pulmonary nodules: Meta-analytic comparison of cross-sectional imaging modalities for diagnosis of malignancy. *Radiology* 246: 772-782, 2008.
3. Wahidi MM, Govert JA, Goudar RK, Gould MK and McCrory DC: American College of Chest Physicians: Evidence for the treatment of patients with pulmonary nodules: When is it breast cancer? ACCP evidence-based clinical practice guidelines. *Chest* 132 (Suppl 3): S94-S107, 2007.
4. Wong N and Wang X: miRDB: An online resource for microRNA target prediction and functional annotations. *Nucleic Acids Res* 43 (Database Issue): D146-D152, 2015.
5. Herder GJ, van Tinteren H, Golding RP, Kostense PJ, Comans EF, Smit EF and Hoekstra OS: Clinical prediction model to characterize pulmonary nodules: Validation and added value of 18F-fluorodeoxyglucose positron emission tomography. *Chest* 128: 2490-2496, 2005.
6. Kim SH, Cho YR, Kim HJ, Oh JS, Ahn EK, Ko HJ, Hwang BJ, Lee SJ, Cho Y, Kim YK, *et al*: Antagonism of VEGF-A-induced increase in vascular permeability by an integrin $\alpha\beta 1$ -Shp-1-cAMP/PKA pathway. *Blood* 120: 4892-4902, 2012.
7. Yanokura M, Banno K, Kobayashi Y, Kisu I, Ueki A, Ono A, Masuda K, Nomura H, Hirasawa A, Susumu N and Aoki D: MicroRNA and endometrial cancer: Roles of small RNAs in human tumors and clinical applications (Review). *Oncol Lett* 1: 935-940, 2010.

8. Engels BM and Hutvagner G: Principles and effects of microRNA-mediated post-transcriptional gene regulation. *Oncogene* 25: 6163-6169, 2006.
9. Philippe L, Alsaleh G, Bahram S, Pfeffer S and Georgel P: The miR-17~92 cluster: A key player in the control of inflammation during rheumatoid arthritis. *Front Immunol* 4: 70, 2013.
10. Dylla L, Moore C and Jedlicka P: MicroRNAs in Ewing sarcoma. *Front Oncol* 3: 65, 2013.
11. Renner W, Kotschan S, Hoffmann C, Obermayer-Pietsch B and Pilger E: A common 936 C/T mutation in the gene for vascular endothelial growth factor is associated with vascular endothelial growth factor plasma levels. *J Vasc Res* 37: 443-448, 2000.
12. Wolf G, Aigner RM, Schaffler G, Langsenlehner U, Renner W, Samonigg H, Yazdani-Biuki B and Kripl P: The 936C> T polymorphism of the gene for vascular endothelial growth factor is associated with 18F-fluorodeoxyglucose uptake. *Breast Cancer Res Treat* 88: 205-208, 2004.
13. Bae SJ, Kim JW, Kang H, Hwang SG, Oh D and Kim NK: Gender-specific association between polymorphism of vascular endothelial growth factor (VEGF 936 C>T) gene and colon cancer in Korea. *Anticancer Res* 28: 1271-1276, 2008.
14. Li J, Li L, Li Z, Gong G, Chen P, Liu H, Wang J, Liu Y and Wu X: The role of miR-205 in the VEGF-mediated promotion of human ovarian cancer cell invasion. *Gynecol Oncol* 137: 125-133, 2015.
15. Wang L, Shan M, Liu Y, Yang F, Qi H, Zhou L, Qiu L and Li Y: miR-205 suppresses the proliferative and migratory capacity of human osteosarcoma Mg-63 cells by targeting VEGFA. *Oncotargets Ther* 16: 2635-2642, 2015.
16. Leng S, Bernauer AM, Zhai R, Tellez CS, Su L, Burki EA, Picchi MA, Stidley CA, Crowell RE, Christiani DC and Belinsky SA: Discovery of common SNPs in the miR-205/200 family-regulated epithelial to mesenchymal transition pathway and their association with risk for non-small cell lung cancer. *Int J Mol Epidemiol Genet* 2: 145-155, 2011.
17. Livak KJ and Schmittgen TD: Analysis of relative gene expression data using real-time quantitative PCR and the 2(-Delta Delta C(T)) method. *Methods* 25: 402-408, 2001.
18. Carthew RW and Sontheimer EJ: Origins and mechanisms of miRNAs and siRNAs. *Cell* 136: 642-655, 2009.
19. Schmittgen TD: Regulation of microRNA processing in development, differentiation and cancer. *J Cell Mol Medicine* 12: 1811-1819, 2008.
20. Rosenfeld N, Aharonov R, Meiri E, Rosenwald S, Spector Y, Zepeniuk M, Benjamin H, Shabes N, Tabak S, Levy A, *et al*: MicroRNAs accurately identify cancer tissue origin. *Nat Biotechnol* 26: 462-469, 2008.
21. Croce CM: Causes and consequences of microRNA dysregulation in cancer. *Nat Rev Genet* 10: 704-714, 2009.
22. Mathé EA, Nguyen GH, Bowman ED, Zhao Y, Budhu A, Schetter AJ, Braun R, Reimers M, Kumamoto K, Hughes D, *et al*: MicroRNA expression in squamous cell carcinoma and adenocarcinoma of the esophagus: Associations with survival. *Clin Cancer Res* 15: 6192-6200, 2009.
23. Kimura S, Naganuma S, Susuki D, Hirono Y, Yamaguchi A, Fujieda S, Sano K and Itoh H: Expression of microRNAs in squamous cell carcinoma of human head and neck and the esophagus: miR-205 and miR-21 are specific markers for HNSCC and ESCC. *Oncol Rep* 23: 1625-1633, 2010.
24. Ferrara N: VEGF and the quest for tumour angiogenesis factors. *Nat Rev Cancer* 2: 795-803, 2002.
25. Takahashi S: Vascular endothelial growth factor (VEGF), VEGF receptors and their inhibitors for antiangiogenic tumor therapy. *Biol Pharm Bull* 34: 1785-1788, 2011.
26. Omuro AM, Faivre S and Raymond E: Lessons learned in the development of targeted therapy for malignant gliomas. *Mol Cancer Ther* 6: 1909-1919, 2007.
27. Thomas G, Jacobs KB, Kraft P, Yeager M, Wacholder S, Cox DG, Hankinson SE, Hutchinson A, Wang Z, Yu K, *et al*: A multistage genome-wide association study in breast cancer identifies two new risk alleles at 1p11.2 and 14q24.1 (RAD51L1). *Nat Genet* 41: 579-584, 2009.
28. Goldstein DB: Common genetic variation and human traits. *N Engl J Med* 360: 1696-1698, 2009.
29. Esquela-Kerscher A and Slack FJ: Oncomirs-microRNAs with a role in cancer. *Nat Rev Cancer* 6: 259-269, 2006.
30. Chen K and Rajewsky N: Natural selection on human microRNA binding sites inferred from SNP data. *Nat Genet* 38: 1452-1456, 2006.
31. Bartel DP: MicroRNAs: Genomics, biogenesis, mechanism, and function. *Cell* 116: 281-297, 2004.
32. Iorio MV, Ferracin M, Liu CG, Veronese A, Spizzo R, Sabbioni S, Magri E, Pedriali M, Fabbri M, Campiglio M, *et al*: MicroRNA gene expression deregulation in human breast cancer. *Cancer Res* 65: 7065-7070, 2005.
33. Duan R, Pak C and Jin P: Single nucleotide polymorphism associated with mature miR-125a alters the processing of pri-miRNA. *Hum Mol Genet* 16: 1124-1131, 2007.
34. Abelson JF, Kwan KY, O'Roak BJ, Baek DY, Stillman AA, Morgan TM, Mathews CA, Pauls DL, Rasin MR, Gunel M, *et al*: Sequence variants in SLITRK1 are associated with Tourette's syndrome. *Science* 310: 317-320, 2005.
35. Landi D, Gemignani F, Barale R and Landi S: A catalog of polymorphisms falling in microRNA-binding regions of cancer genes. *DNA Cell Biol* 27: 35-43, 2008.
36. He H, Jazdzewski K, Li W, Liyanarachchi S, Nagy R, Volinia S, Calin GA, Liu CG, Franssila K, Suster S, *et al*: The role of microRNA genes in papillary thyroid carcinoma. *Proc Natl Acad Sci USAmerica* 102: 19075-19080, 2005.
37. Domigan CK, Warren CM, Antanesian V, Happel K, Ziyad S, Lee S, Krall A, Duan L, Torres-Collado AX, Castellani LW, *et al*: Autocrine VEGF maintains endothelial survival through regulation of metabolism and autophagy. *J Cell Sci* 128: 2236-2248, 2015.